Structural thermal adaptation of β-tubulins from the Antarctic psychrophilic protozoan Euplotes focardii

ARTICLE *in* PROTEINS STRUCTURE FUNCTION AND BIOINFORMATICS · APRIL 2012

Impact Factor: 2.63 · DOI: 10.1002/prot.24016 · Source: PubMed

6 AUTHORS, INCLUDING:

Federica Chiappori
Italian National Research Council
12 PUBLICATIONS **83** CITATIONS
SEE PROFILE

Ivan Merelli
Italian National Research Council
91 PUBLICATIONS **481** CITATIONS
SEE PROFILE

Patrizia Ballarini
University of Camerino
35 PUBLICATIONS **538** CITATIONS
SEE PROFILE

Cristina Miceli
University of Camerino
76 PUBLICATIONS **1,159** CITATIONS
SEE PROFILE

PROTEINS
STRUCTURE ■ FUNCTION ■ BIOINFORMATICS

Structural thermal adaptation of β-tubulins from the Antarctic psychrophilic protozoan *Euplotes focardii*

Federica Chiappori,[1*] Sandra Pucciarelli,[2*] Ivan Merelli,[1] Patrizia Ballarini,[2] Cristina Miceli,[2] and Luciano Milanesi[1]

[1] Istituto di Tecnologie Biomediche – Consiglio Nazionale delle Ricerche, Segrate (MI), Italy
[2] Scuola di Bioscienze e Biotecnologie, University of Camerino, Camerino, Italy

ABSTRACT

Tubulin dimers of psychrophilic eukaryotes can polymerize into microtubules at 4°C, a temperature at which microtubules from mesophiles disassemble. This unique capability requires changes in the primary structure and/or in post-translational modifications of the tubulin subunits. To contribute to the understanding of mechanisms responsible for microtubule cold stability, here we present a computational structural analysis based on molecular dynamics (MD) and experimental data of three *β*-tubulin isotypes, named EFBT2, EFBT3, and EFBT4, from the Antarctic protozoon *Euplotes focardii* that optimal temperature for growth and reproduction is 4°C. In comparison to the *β*-tubulin from *E. crassus*, a mesophilic *Euplotes* species, EFBT2, EFBT3, and EFBT4 possess unique amino acid substitutions that confer different flexible properties of the polypeptide, as well as an increased hydrophobicity of the regions involved in microtubule interdimeric contacts that may overcome the microtubule destabilizing effect of cold temperatures. The structural analysis based on MD indicated that all isotypes display different flexibility properties in the regions involved in the formation of longitudinal and lateral contacts during microtubule polymerization. We also investigated the role of *E. focardii β*-tubulin isotypes during the process of cilia formation. The unique characteristics of the primary and tertiary structures of psychrophilic *β*-tubulin isotypes seem responsible for the formation of microtubules with distinct dynamic and functional properties.

Proteins 2012; 00:000–000.

Key words: molecular dynamics; microtubule; isotypes; cilia; ligand effect; structural flexibility; cellular function.

BACKGROUND

Tubulins are highly conserved eukaryotic proteins[1]; dimers of α- and β-subunits polymerize into hollow cylindrical polymers of 13 protofilaments, known as microtubules.[2] Microtubules are the major components, together with actin filaments, of the cytoskeleton. Besides cytoskeleton, microtubules are components of different cellular structures with specific function, such as mitotic spindle, centrioles, basal bodies, and cilia. Microtubule function includes intracellular transport, motility, and cell division. Essential to this function is the microtubule polarity,[1,2] due to the differential exposure of α (− end) and β (+ end) subunits at the ends of the filament.[2] Each tubulin dimer binds two molecules of GTP in a highly conserved binding site: the nucleotide bound to α-tubulin is nonexchangeable, whereas the nucleotide bound to β-tubulin is exchangeable, because the GTP is hydrolyzed to GDP. The β-tubulin-bound GTP is required for microtubule polymerization and it is hydrolyzed after dimer addition to the microtubule end.[2] In particular, there are two models for microtubule elongation process: the *allosteric model*[3] and the *lattice model*.[4] The *allosteric* model postulates that GTP binding to β-tubulin triggers the dimer to assume a straight conformation that is competent to form lateral interactions. Conversely, hydrolysis of β-tubulin-bound GTP to GDP causes the dimer to revert to a curved conformation that is prone to disassembly. The more recent *lattice* model postulates that tubulin adopts the curved conformation independently of the status of the β-tubulin-bound guanine nucleotide. Thus, the conformational changes in the heterodimer during polymerization are the consequence,

Abbreviations: CTD, C-terminal domain; ECBT, *Euplotes crassus* beta tubulin; EFBT2, *Euplotes focardii* beta-tubulin isotype two; EFBT3, *Euplotes focardii* beta-tubulin isotype three; EFBT4, *Euplotes focardii* beta-tubulin isotype four; GDP, guanosine-5′-diphosphate; GTP, guanosine-5′-triphosphate; ID, intermediate domain; MAPs, microtubule-associated proteins; NBD, nucleotide binding domain; RMSD, root mean square deviation; RMSF, root mean square fluctuation.

Grant sponsor: Italian Ministry Education and Research the Flagship "InterOmics," ITALBIONET; Grant number: RBPR05ZK2Z; Grant sponsor: Bioinformatics analysis applied to Populations Genetics; Grant number: RBIN064YAT 003 projects; Grant sponsors: Italian PNRA and MIUR.
Federica Chiappori and Sandra Pucciarelli contributed equally to this work.
*Correspondence to: Federica Chiappori, Istituto di Tecnologie Biomediche – Consiglio Nazionale delle Ricerche, via Fratelli Cervi, 93 20090 Segrate (MI), Italy. E-mail: federica.chiappori@itb.cnr.it (or) Sandra Pucciarelli, Scuola di Bioscienze e Biotecnologie, University of Camerino, Camerino, Italy. E-mail: sandra.pucciarelli@unicam.it.
Received 30 September 2011; Revised 17 November 2011; Accepted 4 December 2011
Published online 22 December 2011 in Wiley Online Library (wileyonlinelibrary.com). DOI: 10.1002/prot.24016

not the cause, of tubulin incorporation into the lattice. The role of GTP in this model is to tune the strength of the microtubule lattice contacts.

Both α- and β-tubulins are 50 KDa proteins with three structurally conserved domains: the nucleotide binding domain (NBD), the intermediate domain (ID) and the C-terminal domain (CTD).[5] The first comprises six parallel β-strands (S1–S6) alternated with six helices (H1–H6); loops (T1–T6) between secondary structures and the N-terminus of H7 are directly involved in the NBD. The ID is composed of three helices (H8–H10) and four β-strands (S7–S10). The CTD comprises two α-helices (H11–H12) that close up to the other domains. This region of the protein lies on the exterior surface of the microtubule and it is the putative binding site for several microtubule-associated proteins (MAPs). In most eukaryotic organisms, both α- and β-tubulins consist of isotypes encoded by different genes and are grouped into classes of vertebrates.[6] Tubulin isotypes vary from each other mainly by differences in the amino acid sequences clustered within the last 15 CTD residues, which constitute the isotype-defining domain.

Generally, in homeothermic animals (organisms that live at temperate environments) the assembly of microtubules from the α- and β-tubulin heterodimers requires physiological temperatures (30–37°C) and those microtubules usually disassemble at temperatures below 4°C. In chronically cold habitats, the microtubule dynamics of psychrophilic organisms most likely reflect adaptive modifications of the microtubule molecular components. In vitro polymerization assays performed with tubulin purified from cold-adapted fishes[7,8] have provided evidence that these modifications are mostly represented by amino acid substitutions in the tubulin subunits which occur post-translationally, whereas an association of microtubules with stabilizing factors seems to be excluded.[8] An organism of interest for case studies of microtubule cold stability is *Euplotes focardii*, a ciliated protozoan endemic of Antarctic coastal seawater, which shows optimal survival and reproduction rates at 4–5°C.[9] *E. focardii* is exceptionally rich in microtubules and up to now one gene encoding for the α-tubulin (GenBank acc. no. AAL73386), and four different genes encoding for β-tubulin, named *EFBT1*, *EFBT2*, *EFBT3*, and *EFBT4* (GenBank acc. no. AAB31932, FJ664406, FJ664407, and FJ66440, respectively), have been characterized.[10–12] The predicted amino acid sequence of EFBT1 and EFBT2 have a sequence identity of 98%, whereas EFBT3 and EFBT4 show a sequence identity with the other two β-tubulins that range between 84% and 89%.[12] Furthermore, differences are localized in the CTD, which lead to the identification of three β-tubulin isotypes. The expression of three different isotypes can be an adaptive strategy of *E. focardii* to use different β-tubulins, each one with peculiar dynamic properties, to form microtubules at the low temperature of the Antarctic environment.[12] Distinct tubulin isotypes may also affect microtubule assembly kinetics by differences in the GTP binding affinity.[13]

In this work, we present a computational structural analysis based on molecular dynamics (MD) and experimental data of the three *E. focardii* β-tubulins isotypes. We investigated the structural adaptation of EFBT2, EFBT3, and EFBT4 and the effect of natural ligands binding, GTP and GDP, at low temperature. To compare structure flexibility and binding effects at different temperatures, EFBT2, EFBT3, and EFBT4 were modeled on the *Bos taurus* structure and were undergone to MD simulations at 4°C to reproduce the living temperature of the Antarctic species, and 27°C as comparison with the living temperature of mesophilic species. Results are interpreted in comparison with the MD simulation of the *B. taurus* structure and of the β-tubulin from *E. crassus*, a congeneric mesophilic marine species, and with their role in ciliogenesis.

METHODS

Purification of tubulin

The purification of MAP-free tubulin from *E. focardii* was performed as described by Detrich et al.[8] *E. focardii* cell cultures (containing approximately 4 millions cells/L) were centrifuged at 500*g* for 5 min, suspended in PEMGT buffer (100 m*M* PIPES-NaOH, 10 m*M* EGTA, 2 m*M* MgCl2, 0.1 m*M* GTP, 2 m*M* TAME, and pH 6.9) containing protease inhibitors (5 m*M* EGTA, 5 m*M* EDTA, 2 m*M* PMSF, 2 m*M* o-phenanthroline, 10 mg/mL pepstatin A, and 5 mg/mL leupeptin), and sonicated three times for 5 s (14/30 amplitude microns, Soniprep 150). The suspension was incubated with $CaCl_2$ (10 m*M* final concentration), on ice for 30 min, to promote the disassembly of cold-stable microtubules. The suspension was centrifuged at 30,000*g* and the supernatant loaded on a DEAE-SepharoseTM (GE Healthcare Life Sciences, Milan, Italy) column (5 mL) equilibrated in PEMGT buffer. Tubulin enriched fractions were eluted by application of PMEGT buffer containing 0.4 M NaCl. Fractions that resulted positive to immunoblotting with β-tubulin antibodies were pooled and concentrated by ultrafiltration (Centricon 30, Amicon, Beverly, MA). GTP was added to the resulting material to a final concentration of 1 m*M* and incubated at 20°C for 30 min, to induce microtubule polymerization. Microtubules were recovered by centrifugation at 30,000*g* for 20 min and the purity of the resulting material was checked by sodium dodecyl sulfate-polyacrylamide gel electrophoresis (SDS-PAGE) analysis [Fig. 1(A)].

SDS-PAGE and protein concentration determination

SDS-PAGE (10% acrylamide) was performed according to the method of Laemmli.[14] Protein concentration was measured by the method of Bradford.[15] Bovine serum albumin was used as the standard.

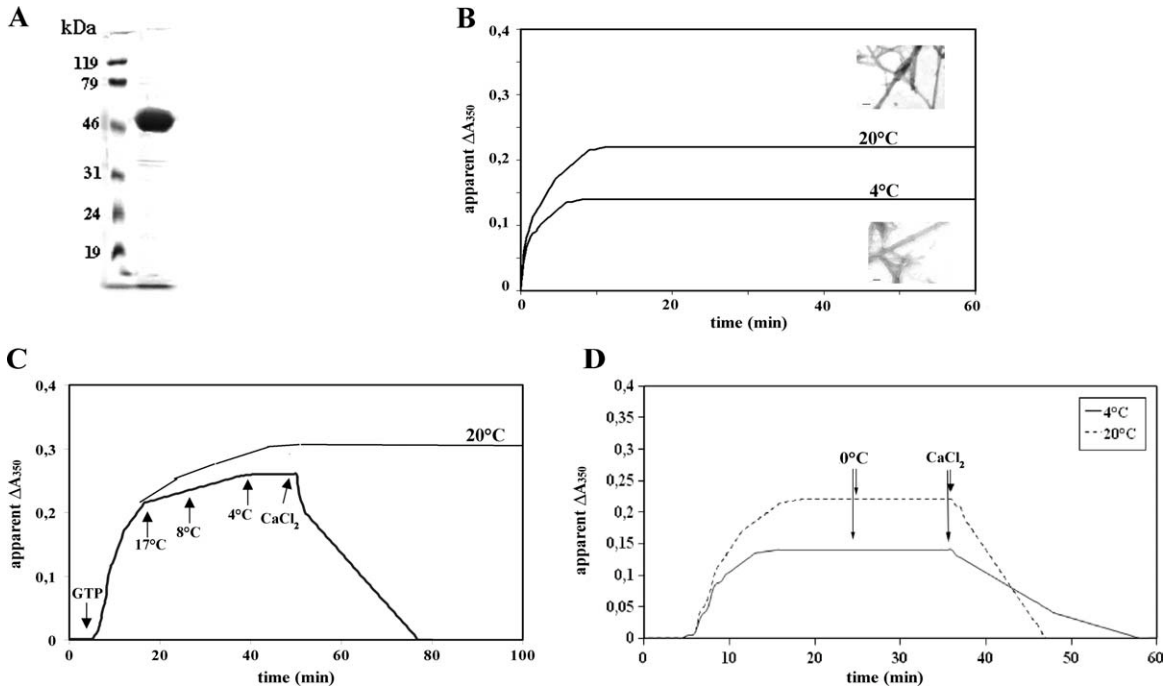

Figure 1

Purification and polymerization of *E. focardii* tubulin. (**A**) *E. focardii* tubulin (3 mg/mL), purified as described under Methods, was analyzed by SDS-PAGE to check the degree of purity. (**B**) Effect of temperature on the polymerization of *E. focardii* tubulin. Polymerization was monitored as change in apparent absorbance at 350 nm (ΔA_{350}). Two samples of purified tubulin (1 mg/mL) at 0°C in the presence of 2 m*M* of GTP, were warmed up to 4°C and to 20°C. Inset: electron micrograph of negatively stained *E. focardii* microtubules withdrawn from the samples at the end of incubation. (**C**) Effect of GTP, cold and calcium ions on polymerization of *E. focardii* tubulin. A sample of purified tubulin (1 mg/mL) at 0°C was warmed up to 20°C. GTP (final concentration 2 m*M*) and $CaCl_2$ (final concentration 10 m*M*) were added at the time as indicated by the arrows. The control sample was maintained at 20°C. At interval (see arrows), the temperature was reduced to the indicated values. (**D**) Effect of the cold on microtubules polymerized at 20°C (dashed line) and 4°C (solid line). Polymerization was started by warming the samples from 0°C to 20°C and 4°C. At the time indicated by the arrow, both samples were cooled to 0°C. Depolymerization was induced by adding $CaCl_2$ to both samples.

Turbidimetric measurement of assembly and electron microscopy

Microtubule assembly was monitored turbidimetrically[16] at 350 nm by means of a Varian Cary1 dual beam spectrophotometer equipped with temperature-controlled multicuvette chambers. For negative-stain electron microscopy, samples from assembly reactions were fixed with aqueous glutaraldehyde [0.8% (w/v)] for 10 min at 0°C. Following fixation, single drops of the sample were applied to carbon-coated grids for 20 sand then stained with one drop of 2% (w/v) aqueous uranyl acetate for 15–20 s. Samples were observed by means of a Philips CM10 transmission electron microscope.

RNA purification

Total RNA was extracted from cultures of *E. focardii* using the RNA Spin Mini RNA Isolation Kit (GE Healthcare, Milan, Italy). Poly(A)$^+$ RNA was purified from *E. focardii* cell cultures (containing approximately 1 million cells/L) using the Quick-Prep® mRNA purification kit (GE Healthcare Life Sciences, Milan, Italy). For cDNA synthesis, the Poly(A)$^+$ RNA (4 μg) was treated with 10 U of RNase-free DNaseI (Bethesda Research Laboratories, MD, USA), in the presence of 40 U of RiboLock® (Fermentas, Milan, Italy) and 4 m*M* $MgCl_2$ for 1 h at 37°C. DNase-treated RNA was incubated with Moloney murine leukemia virus reverse transcriptase (Bethesda Research Laboratories) as recommended by the manufacturer. The resulting first strand cDNA was then precipitated in ethanol, collected by centrifugation, and resuspended in distilled water.

Macronuclear DNA purification, isolation of *E. focardii* β-tubulin nanochromosomes from macronuclear DNA via polymerase chain reaction and rapid amplification of telomeric ends

E. focardii macronuclear DNA was purified as previously described.[10,17] To obtain the gene sequences of *E. focardii* β-tubulin, we performed polymerase chain reaction (PCR) strategies with the oligonucleotides

5′-ATGAGAGAAATTGTACATAT-3′, as forward primer, and 5′-GCGGTGGCATCTTGATATTG-3′, as reverse primer, corresponding to protozoa β-tubulin conserved regions spanning nucleotide 1–20 and 1272–1290, respectively.

E. focardii macronuclear DNA is composed of small nanochromosomes, each usually containing a single gene, which are always terminated by telomeres consisting of four repetitions of the motif C4A4.[18] This stereotypic organization facilitated the achievement of the C-terminal coding region sequences and the 5′- and 3′-UTRs using the Rapid Amplification of Telomeric Ends-PCR (RATE-PCR) technique, as previously described.[10,17] We used as forward primers the oligonucleotides 5′-GGAGAAGGATGGATGAGATG-3′, corresponding to the sequence spanning nucleotides 1200–1219 of the coding region of *E. focardii* β-tubulins in combination with the oligonucleotide 5′-(C4A4)4-3′, containing four repetitions of the motif C4A4 distinctive of the *E. focardii* telomere sequence. To obtain the 5′ noncoding region, we performed the RATE-PCR using as forward primer the oligonucleotide 5′-(C4A4)4-3′, and as reverse primer the oligonucleotide 5′-GCACCAATCTGGTTACCAC-3′, which corresponds to the *E. focardii* β-tubulin sequence spanning nucleotides 35–53. Amplified products were cloned into the pCR2.1-TOPO vector of the TOPO TA Cloning® kit (Invitrogen) following the procedure recommended by the manufacturer. Colony blotting and double-strand DNA labeling, by using the random priming method, were performed according to Sambrook et al.[19] Clones containing β-tubulin recombinant plasmids were sequenced in both strands [ABI Prism sequence analyzer Model 373A and Big Dye Terminator Methodology (PE Applied Biosystems)], whereas EFBT4 tubulin isotype was obtained from a library of macronuclear DNA constructed with the procedure previously described.[11]

Northern blot

Northern blot was performed according to standard procedures on Hybond-N filters (GE Healthcare Life Sciences, Milan, Italy). Filters were prehybridized, hybridized to DNA probes, and washed to remove nonspecifically bound probe according to the manufacturer's recommendations. Filters were stripped for reuse by boiling in distilled water for 15 s.

Deciliation of *E. focardii* cells

Deciliation of *E. focardii* cells was performed by vigorously shaking concentrated cell cultures (containing approximately 700.000 cells/mL) in 4% EtOH/sea water. To recover the cell bodies, cell cultures were incubated for 15 min on ice and then centrifuged at 1100*g* for 3 min. The pellet, composed of cell bodies, was checked by Bright field microscopy to determine the level of deciliation, which typically was ∼90%. Poly(A)$^+$ RNA was purified following the procedure described above, 4 h and 25 h after dilution of deciliated cultures in sea water (to a final cell density of approximately 3000 cells/mL) and incubation at 4°C.

Quantitative real-time PCR

To analyze transcription of the β-tubulin mRNAs, the quantitative real-time PCR (qPCR) protocol was performed using 100 ng of *E. focardii* cDNA prepared from total RNA, using the SYBR green DNA-binding method. The *E. focardii* β-tubulin genes were distinguished by use of the following primer pairs: EFBT2, EfbT2_FW (5′-CTACAACGAAGCCACTGGAG-3′) as forward primer and Efb-T2_REV (5′-GTGACCTTTAGCCCAATTAT-TACC-3′) as reverse primer; EFBT3, EfbT3_FW (5′-GAGTCAGAAGAATGCGATTGTC-3′) as forward primer and Efb-T3_REV (5′-TGGAAAGGGTGGTATTGTATGG-3′) as reverse primer; EFBT4, EfbT4_FW (5′-ATTC-CATTCCCAAGACTCCATTTC-3′) as forward primer and Efb-T4_REV (5′-CAAGGTAGCAGCAGTCAAGTATC-3′). To 100 ng of *E. focardii* cDNA were added 12.5 μL SYBR Premix Ex *Taq* (2×) buffer (TaKaRa Biotech, China), 5 pg of each primer, and water to reach the final volume of 25 μL. The PCR parameters were initial denaturation at 95°C for 2 min to activate the polymerase followed by 45 cycles of denaturation at 95°C for 30 s and annealing and extension at 60°C for 15 s each. Following amplification, melting curve analysis of the DNA was performed at temperatures between 50°C and 95°C, with the temperature increasing at a rate of 0.5°C/10 s. All PCR reactions were performed in a Multicolor qPCR Detection System iCycleriQ (Bio-Rad, Milan, Italy).[17] During the primer annealing/extension step, the increase in the fluorescence from the amplified cDNA was recorded by using the SYBR Green optical channel set at a wavelength of 495 nm. The initial threshold value was set at 30 fluorescent units.

Tubulin isotypes modeling

The MODELLER[20] routine "*multiple_template_model*" and "*multiple_template_evaluation*" were used to obtain, by means of homology modeling, five different models for each β-tubulin sequence. The best models were evaluated according to the DOPE score,[21] from the MODELLER routine, and the Q-MEAN,[22] included in the "*Structure Assessment*" tool of the Swiss-Model server.[23]

Molecular dynamics

MD simulations of β-tubulin complexes were performed with GROMACS 4.0[24] using the GROMOS96 43a1 force field. Complexes were placed in a triclinic

box of SPC water molecules; box dimensions for the three β-tubulin models are 12 nm × 10 nm × 8 nm with about 27,800 water molecules, whereas for 1JFF were 9 nm × 12 nm × 8 nm with about 24,500 water molecules. Counter ions were added at random positions to neutralize protein–ligand total charge, in particular in GDP complexes were added between 28 and 32 Na^+ ions, whereas in the corresponding GTP complexes were added 2 more Na^+ ions. LINCS algorithm[25] was used to constrain bond lengths and periodic boundary conditions were applied in all directions. Van der Waals forces were treated using a cut-off of 12 Å, and long-range electrostatic forces were treated using the Fast Particle-Mesh Ewald method (PME).[26] The simulation time step is 1 fs, and coordinates were saved every 1 ps. Before MD simulations, water molecules were minimized using the Steepest Descent approach until the maximum force was smaller than 10 kJ/mol/nm. Then, the same minimization conditions were applied to side chains and the ligand and finally to the unfixed whole system. The systems were then submitted to two different protocols of Simulated Annealing: the first with temperatures increasing from −273°C to 27°C and the second from −273°C to 4°C in 500 ps. Twenty nanoseconds of MD simulation, conducted in the NVT ensemble at 27°C and 4°C, were obtained for each complex composed by a β-tubulin isotype and GDP or GTP-Mg^{2+}.

Molecules were visualized with VMD[27] and trajectories were analyzed using the GROMACS tools, "*g_rms*" and "*g_rmsf*."

RESULTS

Polymerization properties of *E. focardii* tubulins

To assess the polymerization properties of *E. focardii* tubulins, a turbidimetric analysis of GTP-induced microtubule formation at physiological (4°C) and nonphysiological conditions (20°C) was performed. MAPs-free tubulins purified from *E. focardii* cells [Fig. 1(A)], at a concentration of 1 mg/mL, were warmed up from 0°C to 4°C and from 0°C to 20°C, after the addition of 2 m*M* of GTP. As resulted by turbidimetry analysis [Fig. 1(B)], polymers were formed at both temperatures after 5 min, even though the change in apparent absorbance at 350 nm (apparent ΔA350) was higher at 20°C than at 4°C. Representative electron micrographs of the formed polymers at both temperatures are shown in the inserts of Figure 1(B): in both sample, formed microtubules are composed by 13 protofilaments, and similar in shape and length. The effect of GTP, cold and calcium ions (the last two are considered as microtubule-destabilizing factors) on the polymerization properties of *E. focardii* tubulins were examined, too. Even in this case, polymerization was monitored by the change in apparent absorbance at 350 nm. *E. focardii* tubulin samples were warmed from 0°C to 20°C. As shown in Figure 1(C), the turbidity was increased only after the addition of 2 m*M* GTP to the nucleotide-free samples (see arrow). As the sample temperature was reduced (indicated by the arrows) the turbidity of the solution continued to increase, as the control sample maintained at 20°C, reaching a plateau value at 4°C. A decreasing of turbidity was detected only after the addition of 10 m*M* $CaCl_2$ [see arrow in Fig. 1(C)] to the sample incubated at 4°C, approaching the value observed at time zero. These results demonstrated that pure tubulin from *E. focardii* cells can polymerize *in vitro* to form microtubule at temperatures between 0°C and 20°C, and microtubule formed at 20°C do not depolymerize when incubated at 4°C. Depolymerization of *E. focardii* microtubules was promoted only by the addition of calcium ions to the samples incubated in the cold. The assembly competence and stability in the cold of *E. focardii* tubulins must reflect adaptive changes in tubulin subunits themselves. Finally, we performed a turbidimetric analysis to verify if there is any difference in the sensitivity to cold (0°C) between microtubules polymerized at 4°C and at 20°C [Fig. 1(D)]. We found that depolymerization of both microtubules was promoted at 0°C only by the addition of calcium ions to samples [see arrows in Fig. 1(D)].

To contribute to the understanding of the intrinsic properties of cold stability of the psychrophilic tubulin heterodimers, we investigated the structural adaptation of *E. focardii* β-tubulins isotypes EFBT2, EFBT3, and EFBT4, and the effect of natural ligand bindings, GTP and GDP, by computational molecular dynamic simulation at 4°C and 27°C. The analysis was performed by comparing *E. focardii* and *E. crassus* β-tubulin properties.

Analysis of the *E. focardii* β-tubulin isotype sequences and their role in cilia formation

We determined the nucleotide sequences of the *E. focardii* β-tubulins through multiple strategies: direct isolation of the genes from genomic libraries, and sequence amplification by PCR from genomic DNA and by reverse transcription PCR (mRNA) [see Methods and Refs. 11 and 12]. The alignment of the predicted amino acid sequences from *E. focardii* (EFBT2, EFBT3, and EFBT4) and from *E. crassus* β-tubulins (ECBT in the figure) is shown in Figure 2(A). Gaps are present only at the CTD, the most variable region of tubulin polypeptides. This comparison reveals the presence of 26 nonconservative residue substitutions that are unique to the psychrophile (in black square and Table I). Among the *E. focardii* isotypes, the EFBT2 is the most conserved: it presents only the substitution C232V (*E. crassus* residue/position/*E. focardii* residue), common to all isotypes, localized in the H7 helix. This substitution increases the hydropho-

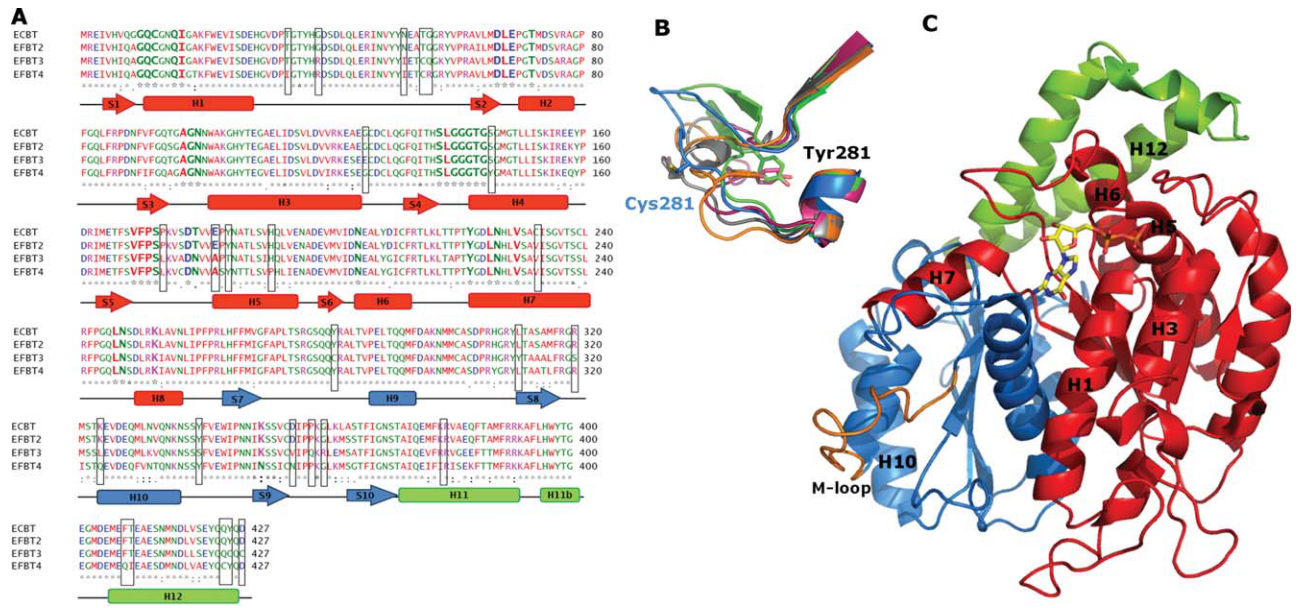

Figure 2

E. focardii β-tubulin substitutions. (**A**) Sequence alignment of *E. focardii* and *E. crassus* β-tubulins used in this study, obtained from ClustalW server. Residues are colored according to their physicochemical properties: red, apolar; green, polar; blue, acidic; pink, basic. Residues composing the binding cavity are in bold. Secondary structures are based on the 1JFF mode: the NBD is colored in red, the ID is in blue, the CTD in green. Residues in black squares are *E. focardii* nonconservative substitutions relative to the *E. crassus* sequence. (**B**) Different conformation of the M-loop in the simulated structures bound to the GDP; in green 1JFF, in gray ECBT, in red, blue and orange EFBT2, EFBT3, and EFBT4, respectively. (**C**) Ribbon diagram of β-tubulin. Secondary structure colors correspond to the domains showed in (A); the M-loop, included in the intermediate domain, is shown in orange, and the GTP molecule is shown in yellow. [Color figure can be viewed in the online issue, which is available at wileyonlinelibrary.com.]

bicity at the interface between NBD and ID. Similar substitutions have also been found in β-tubulins from the Antarctic fishes,[10] thus increased hydrophobicity of tubulins at internal domain interfaces emerges as a common theme for psychrophilic organisms, because microtubule dynamics at low temperature is increased. Considering the binding site, the substitutions S145Y (EFBT4), P173L (EFBT3 and EFBT4), and E181A (EFBT3 and EFBT4) affect residues involved in GTP binding. Among these, the substitution E181A seems particularly significant for cold adaptation, because it is involved in the catalytic mechanism of GTP hydrolysis. Most of the substitutions are grouped in the surface-exposed loops. In particular, R320S (EFBT3), K324L/Q (EFBT3/EFBT4), T33I (EFBT4), D355V/N (EFBT3/EFBT4), and Y425C (EFBT3) are localized in the α/β interface. T33I, K324L, and D355V increase the hydrophobicity in these regions and they may play a key role in the formation of stable *intra-* and *inter*protofilament dimer–dimer interactions during microtubule polymerization in the cold (see Discussion). Other nonconservative substitutions are localized in helices H3, H5, and in the M-loop, involved in lateral contacts between protofilaments [Fig. 2(A–C)]. The substitution H190P, in the H5 helix of EFBT4, modifies one of the residues directly involved in Zn^{2+} binding between protofilaments in zinc-induced tubulin sheets.[5] The EFBT3 has a unique substitution, Y281C, in the M-loop, and two substitutions P358Q and G360R, near the M-loop. The EFBT3 substitution

Table I

Sequence Substitutions in *Euplotes focardii* β-Tubulin Isotypes with Respect to *Euplotes crassus* β-Tubulin

	Longitudinal interaction sites (− end)	Lateral interaction sites		Intradomain interaction surface	GTP/GDP binding site	Taxol binding site	Zn^{2+} contact	Interaction with motor proteins
		M-loop	other					
EFBT2				C232V				
EFBT3	R320S, K324L, D355V	Y281C	G38R, N52I, T55C, G56Q, G126E, L311Y, Y340S	C232V	P173L, E181A, Y183T	P358Q, G360R		K379R, Y425C, D425C
EFBT4	K324Q, D355N		T33I, G38R, N52I, T55C, G56R	C232V	K379I, F408Q, T409I, Q424C		H190P	

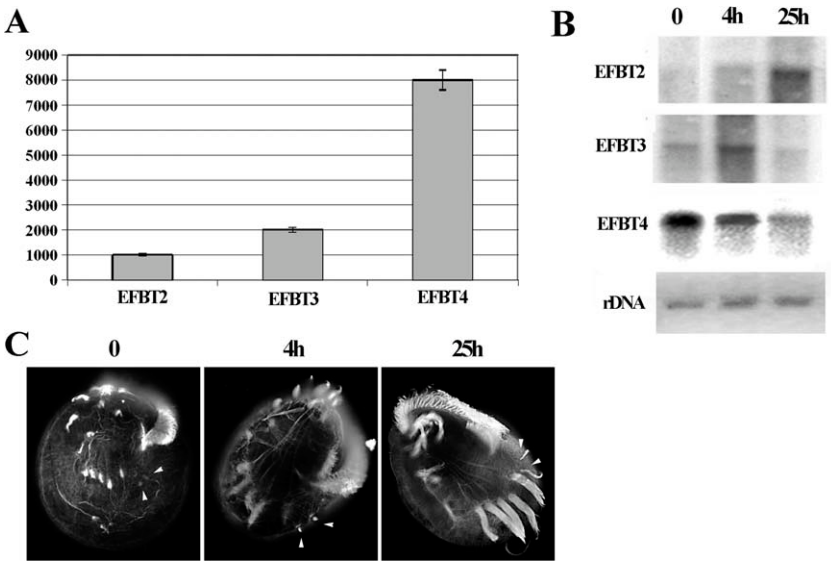

Figure 3

Transcription analysis of the *E. focardii* β-tubulin isotypes. (**A**) β-tubulin isotype transcription level analyzed by quantitative real-time PCR. RNA was extracted from exponentially growing cells. (**B**) Northern blot analysis of Poly(A)$^+$ RNA extracted from *E. focardii* cells 0 h, 4 h, and 25 h after deciliation. Equal amounts of mRNA were analyzed on northern blot hybridized with probes specific of the three different tubulin isotypes. rDNA was used as loading control. (**C**) Fluorescence microscopic images of *E. focardii* cells (ventral views where cilia are fused together to form cirri) stained with an antibody directed against β-tubulin soon after deciliation (Time 0), 4 h after deciliation, and 25 h after deciliation. The complete loss of cilia, the formation of short incomplete cilia, and of complete cilia, is highlighted by arrowheads.

Y281C may play a major role in cold adaptation because, as resulted by our simulation analysis [Fig. 2(C), see below], this substitution determines a different M-loop conformation that exposes the Cys residue outside the tubulin structure, suggesting a direct involvement of this residue in the formation of lateral contacts. The hypothesis that M-loop conformation may play an important role in cold adaptation is supported by the hint that a β-tubulin isotype from the Antarctic fish *Notothenia coriiceps* hold two unique amino acid substitutions (S278G and A283S), which are expected to increase M-loop flexibility.[8] Two substitutions of the EFBT3 isotype are localized in the taxol binding cavity (P358Q and G360R)[28,29]: this cavity is particularly interesting for the inhibition of microtubule formation with antimitotic drugs, albeit mutations that have been reported to confer taxol resistance affect amino acid positions that are distant from the taxol binding cavity.[26,27] Moreover, the substitution P358Q appears particularly important for cold adaptation: the reduction of proline residues is one of the entropic factors included in the structural modifications that affect the psychrophilic enzymes stability.[30] In this contest, it is interesting to note that another substitution, C239S, unique to EFB3 and EFB4, is also present in the human βIII tubulin and it influences the binding of colchicine,[6] suggesting that Ser-239 may have a functional role.[6] The substitutions Q424C (EFBT4), Y425C (EFBT3), and D427C (EFBT3) are localized in the H12 helix, in the CTD, a major site for interaction of tubulin with motor proteins [Fig. 2(A,B)]. The H12 is also involved in the formation of lateral interaction in zinc-induced tubulin sheets. To conclude, most of the substitutions identified in the *E. focardii* β-tubulins replace polar, charged or bulky amino acids with small and neutral/nonpolar ones, as described in literature for psychrophilic enzymes.[31]

Under physiological conditions, all *E. focardii* β-tubulin isotypes are transcribed, but at different extent. As resulted from the qPCR the transcription trend is EFBT4 > EFBT3 > EFBT2 (Fig. 3). To investigate the role of *E. focardii* β-tubulin isotypes in cilia formation, we analyzed the transcription levels of EFBT2, EFBT3, and EFBT4 during reciliation events [Fig. 3(B)]. We extracted Poly(A)$^+$ RNA from *E. focardii* cells before deciliation (0 h), and 4 h and 25 h after deciliation. These time intervals correspond to the formation of short incomplete cilia and of complete cilia, respectively, as resulted by fluorescent microscope analysis using an antibody against β-tubulin [Fig. 3(C)]. Equal amounts of mRNA were analyzed on northern blot and hybridized with probes specific of the three β-tubulin isotypes. As shown in Figure 3(B), the amount of EFBT2 mRNA increased both 4 h and 25 h after deciliation. Contrary, the amount of EFBT3 mRNA increased 4 h after deciliation, but decreased 25 h after deciliation, whereas the EFBT4 mRNA level decreased both 4 h and 25 h after decilia-

tion. This result clearly shows that *E. focardii* β-tubulin isotypes have a different role in cilia regeneration. The EFBT2 isotype is more transcribed in the later event of cilia recovery and therefore appears to be the main component of the cilia. EFBT3 isotype appears stimulated by deciliation suggesting that EFBT3 is involved in the first event of cilia recovery. Contrary, the EFBT4, the most transcribed β-tubulin isotype under physiological condition, appears to be poorly involved in cilia formation because its transcription decreased with the time of reciliation.

Model building

Three-dimensional structures of *E. focardii* and *E. crassus* tubulin are not available, as well as the tubulin structures of other psychrophilic organisms. *B. taurus* (PBD ID: 1JFF_B)[5] and *Sus scrofa* (PDB ID: 1TUB_B)[32] β-tubulin structures present the highest sequence identity with *E. focardii* tubulins, between 80% and 90%. Therefore, *E. focardii* and *E. crassus* β-tubulin models were obtained by homology modeling relying on the 1JFF_B and the 1TUB_B template structures. Five models were achieved for each β-tubulin sequence, among these the best were chosen according the DOPE score value and the Q-MEAN value obtained from Swiss-Model. Differences among the models of the same sequence were localized in the C-terminal region, because the corresponding residues are unsolved in the X-ray structures, and in few regions of nonconserved residues between the two templates. The last 20 residues of the C-terminal region were not included in the final models. The selected models were evaluated in terms of Root Mean Square Deviation (RMSD) respect to 1TUB and 1JFF template structures: the EFBT2 values were 1.7 Å and 3.2 Å, the EFBT3 values were 3.4 Å and 0.8 Å, EFBT4 values were 2.7 Å and 2.2 Å, and ECBT values were 2.2 Å and 2.7 Å, respectively.

MD and simulations stability

Complexes of the four β-tubulin models and 1JFF bound to GDP or GTP-Mg^{2+} were undergone to the minimization protocol described in Material and Methods section and to 20 ns of MD simulation at 27°C and at 4°C. To evaluate the structural stability of the models during the simulation time, the backbone RMSD was calculated with respect to the starting structure (Fig. 4). Trajectories reach the equilibrium in different times. The crystallographic structure 1JFF reached equilibrium in about 2 ns, whereas the β-tubulin models presented an equilibration time between 2 ns and 4 ns at 27°C, and between 1 ns and 5 ns at 4°C. Complexes bound to GDP reached equilibrium in 1–3 ns, whereas complexes with GTP achieved equilibrium in 1–5 ns. No relevant effect of temperature or ligand can be observed. Thus, average RMSD values range between 2.9 Å and 3.7 Å and between 3.1 Å and 4.5 Å for simulations, respectively, at 4°C and 27°C.

Structural flexibility: analysis at different temperatures and comparison of natural ligands effect

To evaluate the differences in structural flexibility in psychrophilic relative to mesophilic β-tubulins, the Root Mean Square Fluctuation (RMSF) values of protein backbone of the equilibrated trajectories portion were calculated. Figure 5(A) shows the effect on tubulin flexibility of the bound nucleotide (GTP or GDP) at the two simulation temperatures of 4°C and 27°C (left and right panels, respectively). Figure 5(B) shows the effect of temperature on GDP or GTP-bound β-tubulin isotypes (left and right panels, respectively). Overall the RMSF plots present similar trends, such as low fluctuations in the secondary structures and high peaks in the loops. The protein portions mainly influenced by temperature and ligand type are the NBD and ID, in particular the loops involved in lateral contacts between protofilaments, such as the M-loop [Fig. 5(A,B), left and right panels]. However, fluctuations localized in the NBD do not concern the loop directly involved in the ligand binding, confirming that these loops belong to a minimal fluctuation region as observed by Keskin et al.[33] The RMSF plots of 1JFF bound to both nucleotide–ligands at 4°C and 27°C are similar, ergo, we exclude relevant temperature influence for GTP or GDP-β-tubulin complexes. The simulations of ECBT bound to GDP presented a higher structural flexibility at 4°C [Fig. 5(A), left panel], whereas bound to GTP no relevant flexibility changes are observable at both temperatures [Fig. 5(B), right panel]. Moreover, mesophilic tubulins bound to GDP or GTP show similar flexibilities at their living temperature. No relevant alterations at H1–S2 loop (residues 12–62), H2 helix (residues 63–68), or M-loop (residues 272–287; H8–H9 loop) are present, in contrast with psychrophilic tubulins (see below). The RMSF curve of complexes EFBT2 displays no relevant changes in flexibility despite the nature of the bound nucleotide (GDP or GTP) and of temperatures (4°C or 27°C). Indeed EFBT2 shows a behavior similar to the mesophilic tubulins. Contrary, EFBT3 and EFBT4 bound to GDP shows relevant differences in RMSF values at 27°C, suggesting a considerable temperature effect on protein flexibility. Furthermore, our analysis reveals that at 4°C the EFBT3 M-loop is more flexible in the GTP-bound state than in the GDP-bound state [Fig. 5(C)]. Considering the involvement of the M-loop in lateral contacts with the H3 helix of the next subunit during microtubule polymerization, a higher flexibility of the M-loop in the GTP-bound EFBT3 would facilitate this process at low temperatures. The unique substitution Y281C (*E. crassus* residue/position/*E. focardii* residue) of

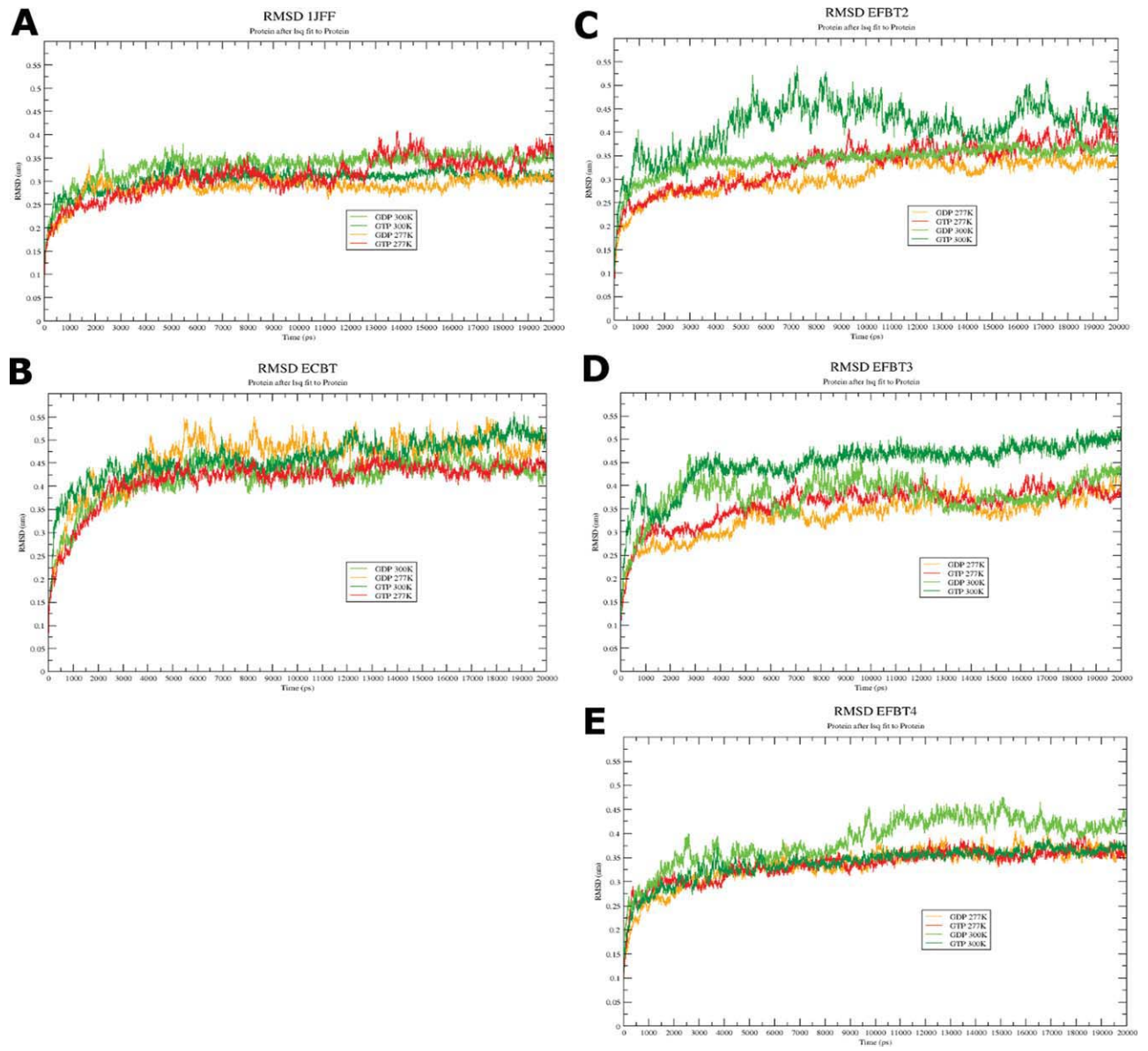

Figure 4

RMSD plot of 1JFF (**A**), ECBT (**B**), EFBT2 (**C**), EFBT3 (**D**), and EFBT4 (**E**) complexes. The Dark green line represents the simulation of β-tubulin bound to GTP at 27°C, the light green corresponds to the simulation of β-tubulin bound to GDP at 27°C, the red line shows the simulation of β-tubulin bound to GTP at 4°C, and the orange line represent the simulation of β-tubulin bound to GDP at 4°C. [Color figure can be viewed in the online issue, which is available at wileyonlinelibrary.com.]

EFBT3 may play a major role in the M-loop flexibility: as revealed by our simulation results, this substitution determines a different loop conformation [Fig. 2(C)]. Besides small differences in the M-loop, a remarkable increase in flexibility is present at 27°C in the GDP-bound state [Fig. 5(A), right panel and Fig. 5(B) left panel] in the H1–S2 loop of EFBT4, involved as well in lateral contacts, and in the H2 helix, that is part of the NBD and is involved in longitudinal interdimeric contacts. Temperature does not have a great influence on the flexibility of mesophilic β-tubulin, whereas psychrophilic β-tubulins result more flexible at 27°C, in particular the EFBT3 bound to GDP. The protein regions mainly affected by temperature or ligand type are the NBD, and the loops involved in longitudinal and lateral contact between protofilaments.

A comparison of the flexibility of secondary structures for each *Euplotes* β-tubulin bound to GDP is shown in Figure 5(C). The bars represent the average RMSF value of the residues included in the secondary structures and in the loops between the secondary structures. This analysis indicates that the *E. focardii* EFBT2 and EFBT3

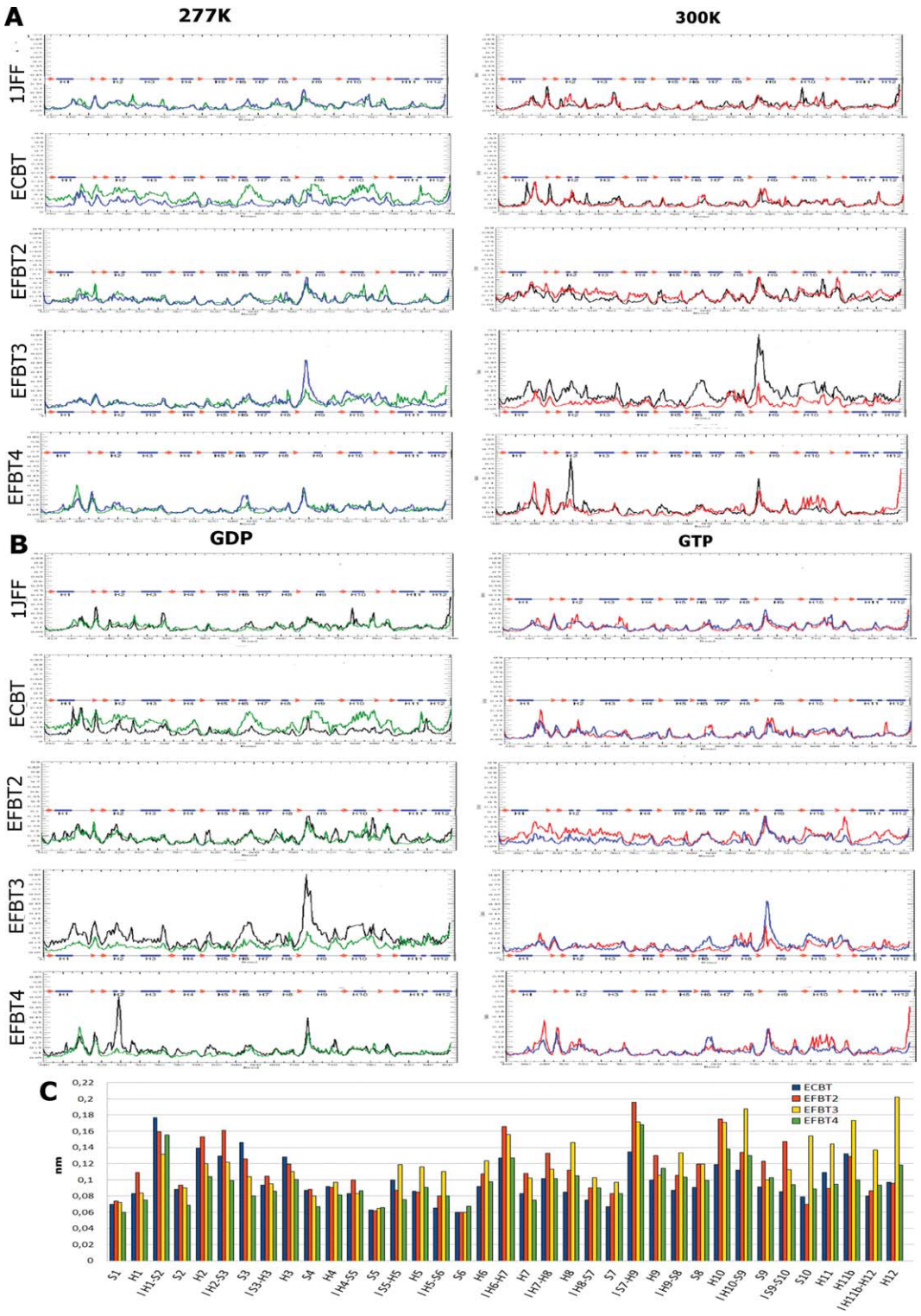

Figure 5

Comparison of RMSF plots of simulations bound to GTP or GDP (**A**), and at 4°C and 27°C (**B**). In each line of the figure one of the β-tubulin complexes is represented: 1JFF, ECBT, EFBT2, EFBT3, and EFBT4; blue and red lines correspond to complexes bound to GTP at 4°C and 27°C, respectively, and green and black line to those bound to GDP at 4°C and 27°C, respectively. (A) Effect of the bound nucleotide at 4°C (left column) and at 27°C (right column); (B) effect of the temperature on GDP-bound tubulins (left column) and on GTP-bound tubulin (right). (**C**) Flexibility of secondary structure comparison. Each bar identifies an element of secondary structure, in blue is represented ECBT, in orange EFBT2, in yellow EFBT3, and in green EFBT4. The height of the bar corresponds to the RMSF average value of the residues in the secondary structure.

isotypes show significant differences in relation to the mesophilic structure of *E. crassus*. All *E. focardii* isotypes show an increased flexibility of the M-loop (loop S7–H9) in relation to the ECBT. EFBT3 display an increased flexibility in secondary structures involved in lateral contacts, that is, H5, H10, and H12, whereas the EFBT4 only in H10 and H12.

DISCUSSION

E. focardii microtubules, as those of all cold-living organisms, must assemble and be stable at the temperatures of the Antarctic Ocean sea waters, which range from −1.8°C to + 1.9°C. In this range of temperature, microtubules of homeotherms normally depolymerize. Our analysis demonstrated that pure tubulin from *E. focardii* cells can polymerize in vitro to form microtubules at temperatures between 4°C and 20°C, and microtubules formed at 20°C did not depolymerize when incubated at 4°C. Depolymerization of *E. focardii* microtubules is promoted only by the addition of calcium ions to the samples incubated in the cold. The assembly competence and stability in the cold of *E. focardii* tubulins must reflect adaptive changes in tubulin subunits themselves, confirming that cold stability of microtubule from psychrophilic organisms resides mainly on intrinsic properties of their tubulin heterodimers, as hypothesized for Antarctic fishes[8] than on the presence of MAPs or dissociable cold-stabilizing ligands. Our turbidimetric analysis and the strict psychrophilic traits of *E. focardii* suggest that its tubulin isotypes are equally cold adapted. However, Panda et al.[34] proposed that one of the mechanism by which cells determine the dynamic properties and functions of microtubules is the alteration of the relative amounts of tubulin isotypes. Therefore, we cannot exclude that *E. focardii* β-tubulin isotypes contribute to the constitution of microtubules with different dynamic properties.

The *E. focardii* β-tubulin substitutions, in comparison to the β-tubulin from *E. crassus*, mapped in regions of the monomer that are involved in lateral contacts between heterodimers and most of them increase the hydrophobicity of these regions. Many charge-to-alanine mutations concentrated at the lateral and longitudinal interfaces between adjacent α- and β-tubulin subunits cause cold sensitivity in yeast.[35] Similarly, the α-tubulin from *E. focardii* contains hydrophobic substitutions that are likely to increase the hydrophobicity of their lateral contact surfaces.[10] A similar increase occurs, through specific amino acid substitutions, also in psychrophilic species of the alga *Chloromonas*.[36] Detrich et al.[8] reported that polymerization of tubulin from Antarctic fishes is under a greater entropic control, in comparison to tubulins from mesophilic species, and that hydrophobic interactions make major contribution to the entropic control of microtubule formation. Indeed, we hypothesize that even in *E. focardii* an increased number of hydrophobic interactions at microtubule interdimeric contacts may overcome the destabilizing effect of low temperatures. The increased hydrophobicity of the substitution C232V (common to all isotypes) may also stabilize the assembly competent conformation of the β-monomer against possible relative rotations of the two domains caused by GTP hydrolysis and may slow the conversion from the straight growing phase to the curved shortening phase of microtubules, during polymerization/depolymerization of microtubules.[3,4] Substitutions that increase the hydrophobicity in this region may also be found in β-tubulins from the Antarctic fishes,[8] and in an equivalent single point mutation in *S. pombe* that affects the dynamics of microtubules making them unable to polymerize in vitro at 4°C.[35] Moreover, the EFBT4 and EFBT3 substitution E181A localized in the nucleotide-binding site most likely change the affinity and exchange rate of GTP. Modifications of β-tubulin residues involved in GTP binding site may change the dynamic of nucleotide hydrolysis stabilizing interdimeric interactions.

MD is a useful tool for the study of thermal adaptation, allowing the identification of regions with differential flexibility involved in the maintenance of biological function at low temperature. Our comparative MD of psychrophilic β-tubulin bound to GDP and GTP, performed at two simulation temperatures, 4°C and 27°C, gives a contribution to elucidate the structural adaptation at low temperature and the effect of NBD on microtubule cold stability. The flexibility of mesophilic β-tubulins is not significantly influenced by temperature. An increase in flexibility is manifested by the *E. crasssus* β-tubulin at 4°C when bound to GDP, which may account for the instability at low temperatures of microtubules from mesophilic organisms. Our results, on the contrary, indicate that the nucleotide state and the temperature influence the flexibility of the psychrophilic β-tubulin portion involved in lateral contacts. However, the effects of these two parameters on the structural flexibility of the three psychrophilic β-tubulin isotypes are different, suggesting that EFBT2, EFBT3, and EFBT4 possess peculiar dynamic properties and that they are involved in distinct cellular functions. For example, the EFBT2 flexibility is only weakly affected by both temperatures and nucleotide. This characteristic and the evidence obtained by the northern blot analysis, wherein EFBT2 expression level increases with the time of reciliation, induce to hypothesize that EFBT2 may be involved in the formation of cilia, microtubular structures that are subjected to a low turnover. The EFBT2 sequence is also the most similar to the mesophilic ECBT (noncold adapted). Furthermore, our analysis revealed that at 4°C the EFBT3 M-loop results more flexible in the GTP-bound state than in the GDP-bound state. This characteristic, and the

result obtained from the Northern blot analysis, where EFBT3 transcription appears activated in the first steps of cilia formation, suggests that the role of EFBT3 is to favor microtubule growing in reciliation. The significant higher flexibility of the M-loop at 4°C when bound to GTP may be important to facilitate the lateral interactions at low temperatures with the β-tubulin of the adjacent protofilament or with the γ-tubulin of the basal bodies during cilia formation. The basal body is a cellular organelle containing γ-tubulin that serves as a nucleation site for the growth of new cilia.[37] Once the tubulin subunit is added to the growing microtubule, the GTP is hydrolyzed to GDP. The M-loop of EFBT3 bound to GDP displays a lower flexibility that may stabilize the basis of the new forming cilium. As revealed by our simulation results [Fig. 2(C)] the unique substitution Y281 in the M-loop of EFBT3 determines a different loop conformation, with Cys residue exposed to the surface, suggesting that it may play a key role in the formation of lateral contacts, and induce to speculate that this cysteine may participate to the coordination of a Zn^{2+} ion. Zinc plays an important role in microtubule dynamics: it reduces the critical concentration of brain tubulins necessary for microtubule assembly and promotes the formation of cold-stable microtubules from tubulins purified from mesophilic organisms.[38] Similarly to EFBT3, EFBT4 presents a higher flexibility of the M-loop and of the loop between H6 and H7 when bound to GTP, whereas bound to GDP, of the loop H1–S2, all involved in lateral contacts. The higher flexibility of the regions involved in longitudinal and lateral contacts can represent an advantage for the formation of cytoskeletal microtubules in the cold, suggesting that it may be involved in the formation of microtubules with a rapid turnover. This hypothesis is in agreement with the results obtained by the northern blot analysis, in which the EFBT4 isotype appears only poorly transcribed during cilia formation, whereas it is the more expressed under physiological conditions suggesting that it may represent the main constituent of intracellular microtubules. In addition, the RMSD values indicate a high structural stability of EFBT4 when bound to both ligands, which may be important for the maintenance of the protein structure at low temperature.

CONCLUSIONS

Our results indicate that in *E. focardii* is present a tubulin pool composed of structurally heterogeneous β-tubulins that may be responsible of the formation of microtubules with different dynamic properties in the cold. The different dynamic properties seem correlated with distinct cellular functions. The EFBT2 displays a lower flexibility compared with other tubulin isotypes, suggesting that it may be the main component of stable microtubules, as cilia. The high flexibility at 4°C of the EFBT3 M-loop, when this isotype is bound to GTP, suggests that it may serve to facilitate the formation of lateral interactions and therefore to drive the first steps of microtubule polymerization in the cold. The EFBT4 possesses regions involved in longitudinal and lateral contacts that are highly flexible, in particular when bound to GDP, suggesting that this isotype may be involved in the formation of very dynamic microtubular structures in the cold.

ACKNOWLEDGMENTS

The authors thank John Hatton of Institute for Biomedical Technologies (ITB-CNR) for proofreading the manuscript.

REFERENCES

1. Nogales E, Downing KH, Amos LA, Löwe J. Tubulin and FtsZ form a distinct family of GTPases. Nat Struct Biol 1998;5:451–458.
2. Tran PT, Joshi P, Salmon ED. How tubulin subunits are lost from the shortening ends of microtubules. J Struct Biol 1997;118:107–118.
3. Desai A, Mitchison TJ. Microtubule polymerization dynamics. Annu Rev Cell Dev Biol 1997;13:83–117.
4. Buey RM, Díaz JF, Andreu JM. The nucleotide switch of tubulin and microtubule assembly: a polymerization-driven structural change. Biochemistry 2006;45:5933–5938.
5. Löwe J, Li H, Downing KH, Nogales E. Refined structure of αβ-tubulin at 3.5 Å resolution. J Mol Biol 2001;313:1045–1057.
6. Joe PA, Banerjee A, Ludueña RF. The roles of cys124 and ser239 in the functional properties of human betaIII tubulin. Cell Motil Cytoskeleton 2008;65:476–486.
7. Wallin M, Strömberg E. Cold-stable and cold-adapted microtubules. Int Rev Cytol 1995;157:1–31.
8. Detrich HW, III, Parker SK, Williams RC, Jr, Nogales E, Downing KH. Cold adaptation of microtubule assembly and dynamics. Structural interpretation of primary sequence changes present in the alpha- and beta-tubulins of Antarctic fishes. J Biol Chem 2000;275:37038–37047.
9. Valbonesi A, Luporini P. Biology of *Euplotes focardii* an Antarctic ciliate. Polar Biol 1990;13:489–493.
10. Pucciarelli S, Miceli C. Characterization of the cold-adapted alpha-tubulin from the psychrophilic ciliate *Euplotes focardii*. Extremophiles 2002;5:385–389.
11. Miceli C, Ballarini P, Di Giuseppe G, Valbonesi A, Luporini P. Identification of the tubulin gene family and sequence determination of one β-tubulin gene in a cold-poikilotherm protozoan, the Antarctic ciliate *Euplotes focardii*. J Eukaryot Microbiol 1994;41:420–427.
12. Pucciarelli S, La TA, Ballarini P, Barchetta S, Yu T, Marziale F, Passini V, Methé B, Detrich HW, III, Miceli C. Molecular cold-adaptation of protein function and gene regulation: the case for comparative genomic analyses in marine ciliated protozoa. Mar Genomics 2009;2:57–66.
13. Huzil JT, Ludueña RF, Tuszynski J. Comparative modeling of human β tubulin isotypes and implications for drug binding. Nanotechnology 2006;17:S90–S100.
14. Laemmli UK. Cleavage of structural proteins during the assembly of the head of bacteriophage T4. Nature 1970;227:680–685.
15. Bradford MM. Rapid and sensitive method for the quantitation of microgram quantities of protein utilizing the principle of protein–dye binding. Anal. Biochem 1976;72:248–254.
16. Detrich HW, III, Jordan MA, Wilson L, Williams RC, Jr. Mechanism of microtubule assembly. Changes in polymer structure and

organization during assembly of sea urchin egg tubulin. J Biol Chem 1985;260:9479–9490.
17. Marziale F, Pucciarelli S, Ballarini P, Melki R, Uzun A, Ilyin VL, Detrich HW, III, Miceli C. Different roles of two γ-tubulin isotypes in the cytoskeleton of the Antarctic ciliate *Euplotes focardii*. FEBS J 2008;275:5367–5382.
18. Hoffman DC, Anderson RC, DuBois ML, Prescott DM. Macronuclear gene-sized molecules of hypotrichs. Nucleic Acids Res 1995;23:1279–83.
19. Sambrook J, Russel DW. Molecular Cloning: A Laboratory Manual, 3rd edn. Cold Spring Harbor Laboratory Press, New York, NY; 2001.
20. Eswar N, Webb B, Marti-Renom MA, Madhusudhan MS, Eramian D, Shen MY, Pieper U, Sali A. Comparative protein structure modeling with MODELLER. Curr Protoc Bioinformatics 2006, Unit 5.6.
21. Shen M, Sali A. Statistical potential for assessment and prediction of protein structures. Protein Sci 2006;15:2507–2524.
22. Benkert P, Tosatto SCE, Schomburg D. QMEAN: a comprehensive scoring function for model quality assessment. Proteins 2008;71:261–277.
23. Arnold K, Bordoli L, Kopp J, Schwede T. The SWISS-MODEL Workspace: a web-based environment for protein structure homology modelling. Bioinformatics 2006;22:195–201.
24. Hess B, Kutzner C, van der Spoel D, Lindahl E. GROMACS 4: algorithms for highly efficient, load-balanced, and scalable molecular simulation. J Chem Theory Coumput 2008;4:435–447.
25. Hess B, Bekker H, Berendsen HJC, Fraaije JGEM: LINCS. A linear constraint solver for molecular simulations. J Comp Chem 1997;18:1463–1472.
26. Essman U, Perera L, Berkowitz ML, Darden T, Lee H, Pedersen LG. A smooth particle mesh ewald potential. J Chem Phys 1995;103:8577–8592.
27. Humphrey W, Dalke A, Schulten K. VMD—visual molecular dynamics. J Mol Graph 1996;14:33–38.
28. Cheung CH, Wu SY, Lee TR, Chang CY, Wu JS, Hsieh HP, Chang JY. Cancer cells acquire mitotic drug resistance properties through beta I-tubulin mutations and alterations in the expression of beta-tubulin isotypes. PLoS One 2010;5:e12564.
29. Yin S, Bhattacharya R, Cabral F. Human mutations that confer paclitaxel resistance. Mol Cancer Ther 2010;9:327–335.
30. Feller G, Gerday C. Psychrophilic enzymes: molecular basis of cold adaptation. Cell Mol Life Sci 1997;53:830–841.
31. Metpally RPR, Reddy BVB. Comparative proteome analysis of psychrophilic versus mesophilic bacterial species: insights into the molecular basis of cold adaptation of proteins. BMC Genomics 2009;10:11.
32. Nogales E, Wolf SG, Downing KH. Structure of the alpha beta tubulin dimer by electron crystallography. Nature 1998;391:199–203.
33. Keskin O, Durell SR, Bahar I, Jernigan RL, Covell DG. Relating molecular flexibility to function: a case study of tubulin. Biophys J 2002;83:663–680.
34. Panda D, Miller HP, Banerjee A, Ludueña RF, Wilson L. Microtubule dynamics in vitro are regulated by the tubulin isotype composition. Proc Natl Acad Sci USA 1994;91:11358–11362.
35. Richards KL, Anders KR, Nogales E, Schwartz K, Downing KH, Botstein D. Structure–function relationships in yeast tubulins. Mol Biol Cell 2000;11:1887–1903.
36. Willem S, Srahna M, Devos N, Gerday C, Loppes R, Matagne RF. Protein adaptation to low temperatures: a comparative study of alpha-tubulin sequences in mesophilic and psychrophilic algae. Extremophiles 1999;3:221–226.
37. Shang Y, Tsao CC, Gorovsky MA. Mutational analyses reveal a novel function of the nucleotide-binding domain of gamma-tubulin in the regulation of basal body biogenesis. J Cell Biol 2005;171:1035–1044.
38. Hesketh JE, Ciesielski-Treska J, Aunis D. Cold-stable microtubules and microtubule-organing centres in astrocytes in primary culture. Neurosci Lett 1984;51:155–160.